Second-order scheme for quadrature-based velocity high order moment methods for disperse two-phase flows

By D. Kah, A. Vié, C. Chalons AND M. Massot

1. Motivation and objectives

The physics of particles and droplets in a carrier gaseous flow field is described in many applications (fluidized beds, spray dynamics, alumina particles in rocket boosters, ...) by a number density function (NDF) satisfying a kinetic equation introduced by (Williams 1958). Solving such a kinetic equation relies either on a sample of discrete numerical parcels of particles through a Lagrangian–Monte-Carlo approach or on a moment approach resulting in a Eulerian system of conservation laws on velocity moments possibly conditioned on size. In the latter case investigated in the present contribution, the main difficulty for particle flows with high Knudsen numbers (i.e., weakly collisional flows), where the velocity distribution can be very far from equilibrium, is the closure of the convective transport at the macroscopic level. One way to proceed is to use quadrature-based moment methods where the higher-order moments required for closure are evaluated from the lower-order transported moments using quadratures in the form of a sum of Dirac delta functions in velocity phase space (see (Yuan & Fox 2011; Kah 2010) and the references therein).

The same problematic has been raised in another component of the literature devoted to multiphase semi-classical limits of the Schrödinger equation. In this context, a series of solutions that converge to measure solutions of the Liouville equation have been characterized. Such an equation can generate multiphase solutions globally in time. Two approaches have been used to solve this equation with a moment approach, either the Heaviside closure (Brenier & Grenier 1998) as it is called in (Jin & Li 2003; Gosse *et al.* 2003), or the one that is related to the present work, the delta closure (see (Jin & Li 2003; Gosse *et al.* 2003) and references therein). It leads to a weakly hyperbolic system of conservation laws by taking moments of a Liouville equation, identical to the Williams-Boltzmann equation studied in gas-particle flows. Such approaches naturally degenerate toward the pressureless gas system of equation in the context of monokinetic velocity distributions (Massot *et al.* 2009; Kah 2010; Runborg 2000).

In our case of interest, quadrature-based or delta closure numerical algorithms have been proposed in Jin & Li (2003); Gosse *et al.* (2003) and Desjardin *et al.* (2008) independently, from (Bouchut *et al.* 2003), using a first order kinetic-based finite volume method. The computation of the cell-centered fluxes by means of the quadrature abscissas and weights ensures realizability and singularity treatment. Such a quadrature approach and the related numerical methods have been shown to be able to capture particle trajectory crossing (PTC) in a direct numerical simulation (DNS) context, where the distribution in the exact kinetic equation remains at all times in the form of a sum of Dirac delta functions. Several attempts have been conducted in order to extend such methods to either partially or fully high-order numerical schemes. In the latter case,

quadrature weights and abscissas for each peak are reconstructed independently (Gosse *et al.* 2003), ensuring conservation of only the zeroth and first-order moments, but not for the higher-order moments, which are very nonlinear functions of abscissas. Although this would not be too critical for smooth solutions, even if not satisfactory, where the dynamics of the two peaks are decorrelated, this would be critical in the description and stability of the method near singularities. On the other hand, partially high-order moment methods introduced in (Vikas *et al.* 2011) ensure conservation of the whole moment set, but introduce high-order only in the weights where the linear character of the dependency allows a simple and efficient quadrature. However, remaining issues prevent the design of a fully high-order transport scheme. The first is related to its ability to preserve the vector of moments inside or at the frontier of the moment space, thus leading to several possibilities of degeneration from a given number of abscissas to a lower integer number. Secondly, in most cases the numerical schemes have to tackle the possibility of singular solutions when the dynamics complexity goes beyond the one allowed by the model. Both issues have been addressed recently in (Chalons *et al.* 2011*b*) in the context of mathematical theory of PDEs and for first-order numerical methods; this has set the background for the design of a fully second order scheme in time and space.

As a next step, this paper introduces a fully second-order in time and space transport scheme for the quadrature-based closure, with linear reconstructions for both weights and abscissas. Whereas realizability is ensured, we suggest an algorithm in order to ensure both conditions: maximum principle for velocity and moment vector conservation, in one or two-dimensional configurations.

The remainder of the paper is organized as follows. The principal features of the model are recalled in section 2. The numerical scheme is explained in section 3 and in section 4, respectively in one and two dimensions. Finally the model is tested in three configurations. The first two, one dimensional, assess the numerical order and highlight the advantage of this scheme compared with a partially second order scheme in case of singularity formation. The last case, a two-dimensional version of the second one, shows that the scheme can be extended to multi-dimensional configurations.

2. Eulerian multi velocity moment model

We recall here the essential results of moment quadrature in a one-dimensional configuration. The complete developments can be found in (Chalons *et al.* 2011*b*).

2.1. *Quadrature*

Consider the solution $f = f(t, x, v)$ of the free transport kinetic equation

$$\partial_t f + v\partial_x f = 0, \quad t > 0,\, x \in \mathbb{R},\, v \in \mathbb{R}, \qquad f(0, x, v) = f_0(x, v). \tag{2.1}$$

The exact solution is given by

$$f(t, x, v) = f(0, x - vt, v) = f_0(x - vt, v).$$

Defining the l-order moment

$$M_l = \int_v f(t, x, v) v^l dv, \quad l = 1, ..., N, \quad N \in \mathbb{N},$$

the associated governing equations are easily obtained from (2.1) after multiplication by v^l and integration over v, and write $\partial_t M_l + \partial_x M_{l+1} = 0$, $l \geq 0$. For the sake of simplicity, but without any restriction, we focus our attention hereafter on the four-moment model,

with $\boldsymbol{M} = (M_0, M_1, M_2, M_3)^t$ and $\mathbf{F}(\boldsymbol{M}) = (M_1, M_2, M_3, \overline{M_4})^t$, and

$$\partial_t \boldsymbol{M} + \partial_x \mathbf{F}(\boldsymbol{M}) = 0. \tag{2.2}$$

This model is closed provided that $\overline{M_4}$ is defined as a function of $\boldsymbol{M}$. In quadrature-based moment methods, the starting point to define this closure relation consists in representing the velocity distribution of $f(t,x,v)$ by a set of two Dirac delta functions, that is a two-node quadrature :

$$f(t,x,v) = \omega_1(t,x)\delta(v - U_1(x,t)) + \omega_2(t,x)\delta(v - U_2(x,t)), \tag{2.3}$$

where the weights $\omega_1(t,x) > 0$, $\omega_2(t,x) > 0$, and the velocity abscissas $U_1(t,x)$, $U_2(t,x)$ are expected to be uniquely determined from the knowledge of $\mathbf{M}(x,t)$. Dropping the (x,t)-dependance to avoid cumbersome notations, such a function f has exact moments of order $i = 0, ..., 4$ given by $\rho_1 U_1^i + \rho_2 U_2^i$. The next step then naturally consists in setting

$$\overline{M_4} = \omega_1 U_1^4 + \omega_2 U_2^4, \tag{2.4}$$

where ω_1, ω_2 and U_1, U_2 are defined from $\boldsymbol{M}$ by the nonlinear system $M_l = \sum_{k=1}^{2} \omega_k U_k^l$.

System (2.2)-(2.4) is well-defined on the convex set Ω, also called the moment space, given by $\Omega = \{\boldsymbol{M} = (M_0, M_1, M_2, M_3)^t, M_0 > 0, M_0 M_2 - M_1^2 > 0\}$. Moreover, setting $\boldsymbol{U} = (\omega_1, \omega_2, \omega_1 U_1, \omega_2 U_2)^t$, the function $\boldsymbol{U} = \boldsymbol{U}(\boldsymbol{M})$ is one-to-one and onto as soon as we set for instance $U_1 > U_2$. Moreover we have $0 < \omega_1 < M_0$ and $0 < \omega_2 < M_0$. This can be extended to the more general case of a $2N$-moment models, $N > 1$. The velocity distribution is represented in this situation by a set of N Dirac delta functions, leading to $M_l = \sum_{k=1}^{N} \omega_k U_k^l$, $l = 0, ..., 2N-1$, and $\overline{M_{2N}} = \sum_{k=1}^{N} \omega_k U_k^{2N}$. The quadrature and the above mentioned proposition are valid at the interior of the moment space. Therefore a thorough study of how to perform the quadrature at the border of the moment space has been done in Chalons *et al.* (2011*b*). We want to be able to switch continuously from two-node to one-node quadrature without pathological behavior on the abscissas and weights. Moreover, when the velocity distribution at the kinetic level has compact support in the initial distribution, such a property (also called maximum principle) will be preserved throughout the dynamics of the system†. Besides, it can be shown that it is naturally verified in one-dimension by the first-order kinetic scheme (Chalons *et al.* 2011*b*).

2.2. *Challenges for a numerical scheme*

In order to write an advection scheme for system (2.2) with a second order reconstruction, two difficulties have to be addressed. First, a maximum principle on velocity arising from system (2.2) has to be enforced. Second, the weights and abscissas affine reconstruction for such a finite volume method needs to be conservative relative to the moment mean values in a cell. Using two single-node quadrature independent reconstructions leads to the conservation of M_0 and M_1. However the nonlinear expression of the higher order moments M_2 and M_3 results into a shift in their means owing to the reconstruction and introduces potential errors and unstable behavior in the singularity treatment where the two quadrature nodes are strongly coupled.

† Such a property can be proved in the context of smooth solution. This comes from the fact that, for system (2.2) (2.4), the abscissas satisfy a transport equation: $\partial_t U_k + U_k \partial_x U_k = 0$, so that $\forall t, \min_x U(0,x) \leq U(t,x) \leq \max_x U(0,x)$ for smooth solutions. Such a property has been proved in the framework of single quadrature pressureless gas dynamics by F. Bouchut but is still a conjecture in the context of multiple quadrature node and related systems

3. One-dimensional second-order numerical scheme

This section is devoted to the discretization of (2.2)-(2.4). Given the conservative nature of the equations, a finite volume scheme appears to be natural. The kinetic-based time solver is first presented, followed by the proposed second order reconstruction.

3.1. *Flux computation via kinetic schemes*

The flux computation uses a kinetic scheme as in (Kah *et al.* 2010; Chalons *et al.* 2011*b*); it is briefly recalled for the sake of completeness.

Let us introduce a time step $\Delta t > 0$ and a space step $\Delta x > 0$ that we assume to be constant for simplicity. We set $\lambda = \Delta t/\Delta x$ and define the mesh interfaces $x_{i+1/2} = i\Delta x$ for $i \in \mathbb{Z}$, and the intermediate times $t^n = n\Delta t$ for $n \in \mathbb{N}$. In the sequel, $\mathbf{M}_j^n$ denotes the approximated average value of $\mathbf{M}$ at time t^n and on the cell $\mathcal{C}_i = [x_{i-1/2}, x_{i+1/2}]$. For $n = 0$, we set $M_{0,i} = \frac{1}{\Delta x}\int_{x_{i-1/2}}^{x_{i+1/2}} M_0 \,\mathrm{d}x$, $i \in \mathbb{Z}$, where $M_0(x)$ is the initial condition. Given $(\boldsymbol{M}_i^n)_{i\in\mathbb{Z}}$ a vector of approximate values at time t^n in Ω, in order to advance to the next time level t^{n+1}, the kinetic scheme is decomposed into two steps. We first set $\boldsymbol{U}_i = \boldsymbol{U}(\boldsymbol{M}_i^n)$ and define the function $(x, v) \to f^n(x, v)$ by

$$f^n(x,v) = \omega_{1,i}^n \delta\big(v - U_{1,i}^n\big) + \omega_{2,i}^n \delta\big(v - U_{2,i}\big), \quad \forall\ (x,v) \in \mathcal{C}_i \times \mathbb{R},\ \ i \in \mathbb{Z}.$$

We then solve the transport equation

$$\begin{cases} \partial_t f + v\,\partial_x f = 0, \quad (x,v) \in \mathbb{R}\times\mathbb{R}, \\ f(t=0,x,v) = f^n(x,v), \end{cases} \tag{3.1}$$

the solution of which is given by $f(t, x, v) = f^n(x - vt, v)$. At last, we set $f^{n+1-}(x, v) = f^n(x - v\Delta t, v)$. Under the natural CFL condition

$$\Delta t \max_{i\in\mathbb{Z}}(U_{1,i}^n, U_{2,i}^n) \le \text{ CFL } \Delta x,$$

with CFL ≤ 1, integrating (3.1) over $(t, x, v) \in (0, \Delta t)\times\mathcal{C}_j\times\mathbb{R}$ and against U^i, $i = 0, ..., 3$ easily leads to the equivalent update formula

$$\boldsymbol{M}_i^{n+1} = \boldsymbol{M}_i^n - \frac{\Delta t}{\Delta x}\big(\boldsymbol{F}_{i+1/2}^n - \boldsymbol{F}_{i-1/2}^n\big), \quad i \in \mathbb{Z},$$

where we us a flux-splitting algorithm where $\boldsymbol{F}_{i+1/2}^n = \boldsymbol{F}_{i+1/2}^{n+} + \boldsymbol{F}_{i+1/2}^{n-}$ and where the flux $\boldsymbol{F}_{i+1/2}^{n\pm}$ writes

$$\boldsymbol{F}_{i+1/2}^{n+} = \frac{1}{\Delta t}\int_0^{+\infty}\int_0^{\Delta t} \boldsymbol{\mathcal{U}} f(\xi, x_{i+1/2}, v)\, v \,\mathrm{d}\xi\mathrm{d}v,\ \ \boldsymbol{F}_{i+1/2}^{n-} = \frac{1}{\Delta t}\int_{-\infty}^{0}\int_0^{\Delta t} \boldsymbol{\mathcal{U}} f(\xi, x_{i+1/2}, v)\, v \,\mathrm{d}\xi\mathrm{d}v, \tag{3.2}$$

where $\boldsymbol{\mathcal{U}} = (1, v, v^2, v^3)^t$. Applying the classical change of variable performed in (Bouchut *et al.* 2003), the final expression of the flux, with $\boldsymbol{\mathcal{U}}_k = (1, U_k, (U_k)^2, (U_k)^3)^t$, writes

$$\boldsymbol{F}_{i+1/2}^{n-} = -\frac{1}{\Delta t}\sum_{k=1}^{2}\left(\int_{x_{i+1/2}}^{x_{i+1/2}-d_{rk}} U_k \boldsymbol{\mathcal{U}}_k(x)\,\omega_k(x)\,\mathrm{d}x\right), \boldsymbol{F}_{i+1/2}^{n+} = \frac{1}{\Delta t}\sum_{k=1}^{2}\left(\int_{x_{i+1/2}-d_{lk}}^{x_{i+1/2}} U_k \boldsymbol{\mathcal{U}}_k(x)\,\omega_k(x)\,\mathrm{d}x\right),$$

where d_{lk} and d_{rk} respectively write, with $U_k^+ = \max(U_k, 0)$, $U_k^- = \min(U_k, 0)$:

$$d_{lk} = \Delta t\frac{U_k^+(x_{i+1/2})}{1 + \Delta t D_{U_{1,i}}}, \quad d_{rk} = \Delta t\frac{U_k^-(x_{i+1/2})}{1 + \Delta t D_{U_{1,i+1}}}.$$

Considering a first order spatial reconstruction, the flux writes

$$\boldsymbol{F}^{n\pm}_{i+1/2} = \left(M^n_{1,i+1/2}, M^n_{2,i+1/2}, M^n_{3,i+1/2}, M^n_{4,i+1/2}\right)^t, \quad M^n_{l,i+1/2} = M^{n-}_{l,i+1/2} + M^{n+}_{l,i+1/2},$$

with $M^{n-}_{l,i+1/2} = \sum_{k=1}^{2} \omega^n_{k,i+1} U^{n-}_{k,i+1} (U^n_{k,i+1})^{l-1}$, and $M^{n+}_{l,i+1/2} = \sum_{k=1}^{2} \omega^n_{k,i} U^{n+}_{k,i} (U^n_{k,i})^{l-1}$.

It is easy to see that this scheme is conservative and preserves the moment space Ω, see for instance (Desjardin *et al.* 2008). Moreover, provided the set of abscissas computed from the quadrature respects the maximum principle, it is further ensured by the scheme. However, a first order scheme is limited in terms of numerical accuracy. To increase the precision and thus avoid the use of refined meshes leading to expensive computations, one needs to increase the order of the scheme.

3.2. *Second-order reconstruction*

The novelty of this paper is to exhibit a fully second order scheme, i.e. with linear reconstruction applying to the weights and the abscissas. Therefore, it goes further in complexity than the scheme proposed in (Vikas *et al.* 2011) where the weights alone are linearly reconstructed, the abscissas being constant. Because the moments are linear in the weights, the conservation of the spatial averages through the reconstruction process is easily obtained in such cases.

Given the value of the moment vector in a cell $\boldsymbol{M}_i = (M_{0,i}, M_{1,i}, M_{2,i}, M_{3,i})$, the corresponding set of weights and abscissas writes: $\omega_{1,i}, \omega_{2,i}, U_{1,i}, U_{2,i}$. In the context of a linear reconstruction, the weights and abscissas write

$$\begin{aligned} \omega_k(x) &= \omega_{k,i} + \Delta\omega_{k,i} + D_{\omega_{k,i}}(x - x_i), \\ U_k(x) &= U_{k,i} + \Delta U_{k,i} + D_{U_{k,i}}(x - x_i) + \Delta^0 U_{k,i}. \end{aligned} \tag{3.3}$$

In system (3.3), the terms X_i represent the mean cell value and D_{X_i} the slope of the quantity X. A minmod limiter is used for the slopes computed from neighbors determined by the convention $U_1 \geq U_2$, so that their expressions are

$$\begin{aligned} D_{\omega_{k,i}} &= \frac{1}{2}\left(sgn(\omega_{k,i+1} - \omega_{k,i}) + sgn(\omega_{k,i} - \omega_{k,i-1})\right) \min\left[\frac{\omega_{k,i+1} - \omega_{k,i}}{\Delta x}\right., \\ &\quad \left.\frac{\omega_{k,i} - \omega_{k,i-1}}{\Delta x}, \frac{2\omega_{k,i}}{\Delta x}\right], \\ D_{U_{k,i}} &= \frac{1}{2}\left(sgn(U_{k,i+1} - U_{k,i}) + sgn(U_{k,i} - U_{k,i-1})\right) \min\left[\frac{U_{k,i+1} - U_{k,i}}{\Delta x(1 - D_{\omega_{k,i}}\Delta x/(6\omega_{k,i}))}\right., \\ &\quad \left.\frac{U_{k,i} - U_{k,i-1}}{\Delta x(1 + D_{\omega_{k,i}}\Delta x/(6\omega_{k,i}))}, \frac{2U_{k,i}}{\Delta x}\right]. \end{aligned}$$

These terms are classical in such a reconstruction. The term $\Delta^0 U$ appearing in the abscissa equations represents the correction added to U_i for the reconstruction to be conservative in the case where the distribution is mono-modal. In this case, the system reduces to the pressureless gas dynamics, with a unique velocity, and $\Delta^0 U$ is the correction brought to U_i (Bouchut *et al.* 2003):

$$\Delta^0 U_{k,i} = \frac{D_{\omega_{k,i}} D_{U_{k,i}} \Delta x^2}{12\omega^2_{k,i}}. \tag{3.4}$$

This correction of the mean value ensures that the spatial averages for M_0 and M_1 are

preserved, but is not sufficient for higher-order moments, such as M_2 and M_3, which require further corrections. For the sake of legibility, let us write

$$\begin{aligned}
&\tilde{\omega}_{1,i} = \omega_{1,i} + \Delta\omega_{1,i}, && \tilde{\omega}_{2,i} = \omega_{2,i} + \Delta\omega_{2,i},\\
&\overline{U_{1,i}} = U_{1,i} + \Delta^0 U_{1,i}, && \overline{U_{2,i}} = U_{2,i} + \Delta^0 U_{2,i}.\\
&\tilde{U}_{1,i} = U_{1,i} + \Delta U_{1,i} + \Delta^0 U_{1,i}, && \tilde{U}_{2,i} = U_{2,i} + \Delta U_{2,i} + \Delta^0 U_{2,i}.
\end{aligned} \tag{3.5}$$

In order to ensure conservation of the whole set, the corrections ΔX_i must be evaluated. These terms are solved by writing the non linear system of equations for the conservation of the four moments:

$$M_{l,i} \;=\; \tfrac{1}{\Delta x}\int_{x_{i-1/2}}^{x_{i+1/2}} \sum_{k=1}^{2} (\tilde{\omega}_{k,i} + D_{\omega_{k,i}}(x - x_i))(\tilde{U}_{k,i} + D_{U_{k,i}}(x - x_i))^l, \quad l = 0 \ldots 3. \tag{3.6}$$

After some algebra, the system of equations reduces to

$$\begin{aligned}
\sum_{k=1}^{2} \tilde{\omega}_{k,i} &= \sum_{k=1}^{2} \omega_{k,i}, \qquad \sum_{k=1}^{2} \tilde{\omega}_{k,i}\tilde{U}_{k,i} = \sum_{k=1}^{2} \omega_{k,i}U_{k,i},\\
\sum_{k=1}^{2} \tilde{\omega}_{k,i}(\tilde{U}_{k,i})^2 &= \sum_{k=1}^{2} \omega_{k,i}U_{k,i}^2 + \tilde{\omega}_{k,i}\tfrac{\Delta x^2}{12}(D_{\omega_{k,i}})^2 + \tilde{\omega}_{k,i}\tfrac{\Delta x^2}{12}(D_{\omega_{k,i}})^2,\\
\sum_{k=1}^{2} \tilde{\omega}_{k,i}(\tilde{U}_{k,i})^3 &= \sum_{k=1}^{2} \omega_{k,i}U_{k,i}^3 - (\tilde{U}_{k,i})^2\tfrac{\Delta x^2}{4}D_{\omega_{k,i}}D_{U_{1,i}} - \tilde{\omega}_{k,i}\tilde{U}_{k,i}\tfrac{\Delta x^2}{4}(D_{U_{1,i}})^2
\end{aligned}$$

The system can be solved by direct Newton algorithm, which has been implemented. However, a modified method can be envisioned that is somewhat simpler and involves a series of matrix-vector products and no inversion. We approximate the system by

$$\boldsymbol{M}_i(\tilde{\boldsymbol{\delta}}_i) = \boldsymbol{M}_i(\boldsymbol{\delta}_i) + \Delta\boldsymbol{M}_i(\tilde{\boldsymbol{\delta}}_i) \tag{3.7}$$

where, in system (3.2), $\boldsymbol{M}_i(\tilde{\boldsymbol{\delta}}_i)$ corresponds to the left-hand side, $\boldsymbol{M}_i(\boldsymbol{\delta}_i)$ to the first term of right-hand side, $\Delta\boldsymbol{M}_i$ to the remaining terms in the right-hand side as a function of $\tilde{\boldsymbol{\delta}}_i = (\tilde{\omega}_{1,i}, \tilde{\omega}_{2,i}, \tilde{U}_{1,i}, \tilde{U}_{2,i})^t$. Because we expect the corrections to be small perturbations around the vector $\boldsymbol{\delta}_i = (\omega_{1,i}, \omega_{2,i}, \overline{U_{1,i}}, \overline{U_{2,i}})^t$, the linearization consists in approximating $\Delta\boldsymbol{M}_i(\tilde{\boldsymbol{\delta}}_i)$ by $\Delta\boldsymbol{M}_i(\boldsymbol{\delta}_i)$ and to write a linearized inversion algorithm

$$\tilde{\boldsymbol{\delta}}_i - \boldsymbol{\delta}_i = (\partial_{\boldsymbol{M}}\boldsymbol{\delta})_i\Delta\boldsymbol{M}_i = (\partial_{\boldsymbol{\delta}}\boldsymbol{M})_i^{-1}\Delta\boldsymbol{M}_i, \tag{3.8}$$

where $\tilde{\boldsymbol{\delta}}_i - \boldsymbol{\delta}_i = (\Delta\omega_{1,i}, \Delta\omega_{2,i}, \Delta U_{1,i}, \Delta U_{2,i})^t$ and with (without cell index for the sake of legibility) a matrix that is evaluated once

$$(\partial_{\boldsymbol{\delta}}\boldsymbol{M})^{-1} = \begin{pmatrix}
\frac{(3\overline{U_1} - \overline{U_2})\overline{U_2}^2}{(\overline{U_1} - \overline{U_2})^3} & -\frac{6\overline{U_1}\,\overline{U_2}}{(\overline{U_1} - \overline{U_2})^3} & \frac{3(\overline{U_1} + \overline{U_2})}{(\overline{U_1} - \overline{U_2})^3} & -\frac{2}{(\overline{U_1} - \overline{U_2})^3}\\
\frac{(\overline{U_1} - 3\overline{U_2})\overline{U_1}}{(\overline{U_1} - \overline{U_2})^3} & \frac{6\overline{U_1}\,\overline{U_2}}{(\overline{U_1} - \overline{U_2})^3} & -\frac{3(\overline{U_1} + \overline{U_2})}{(\overline{U_1} - \overline{U_2})^3} & \frac{2}{(\overline{U_1} - \overline{U_2})^3}\\
-\frac{\overline{U_1}\,\overline{U_2}^2}{\omega_1(\overline{U_1} - \overline{U_2})^2} & \frac{(2\overline{U_1} + \overline{U_2})\overline{U_2}}{\omega_1(\overline{U_1} - \overline{U_2})^2} & -\frac{\overline{U_1} + 2\overline{U_2}}{\omega_1(\overline{U_1} - \overline{U_2})^2} & \frac{1}{\omega_1(\overline{U_1} - \overline{U_2})^2}\\
-\frac{\overline{U_2}\,\overline{U_1}^2}{\omega_2(\overline{U_1} - \overline{U_2})^2} & \frac{(2\overline{U_2} + \overline{U_1})\overline{U_2}}{\omega_2(\overline{U_1} - \overline{U_2})^2} & -\frac{\overline{U_2} + 2\overline{U_1}}{\omega_2(\overline{U_1} - \overline{U_2})^2} & \frac{1}{\omega_2(\overline{U_1} - \overline{U_2})^2}
\end{pmatrix}.$$

We define then the following iterative scheme, for $k \geq 1$, with $\tilde{\boldsymbol{\delta}}_i^0 = \boldsymbol{\delta}_i$ and $\tilde{\boldsymbol{\delta}}_i^1 = \tilde{\boldsymbol{\delta}}_i$:

$$\tilde{\boldsymbol{\delta}}_i^{k+1} = \tilde{\boldsymbol{\delta}}_i^k + (\partial_{\boldsymbol{\delta}} \boldsymbol{M})^{-1} \left(\Delta \boldsymbol{M}_i(\tilde{\boldsymbol{\delta}}_i^k) - \Delta \boldsymbol{M}_i(\tilde{\boldsymbol{\delta}}_i^{k-1}) \right). \tag{3.9}$$

The convergence of this algorithm is observed to be quick and as few as one to three iterations are enough to obtain a converged solution and to preserve strict conservation of moments in the scheme. In the numerical cases presented in the following both the full Newton and this more efficient method have been tested and lead to the same solutions. This algorithm has to be efficient because, once we get the corrected values, we have to eventually go through a test in order to check that the maximum principle is verified by the corrected expressions of the velocities. In the cells where the test is negative, slopes are recomputed in order not to generate any local extremum and enforce the maximum principle. New corrected values with the new velocity slope values are determined through (3.9) until the maximum principle is satisfied everywhere.

4. Two-dimensional second-order numerical scheme

In two-dimensions, the CQMOM quadrature is used (Yuan & Fox 2011):

$$f(t, \mathbf{x}, \mathbf{v}) = \sum_{k=1}^{2} \sum_{l=1}^{2} w_{k,l} \delta(u - U_k) \delta(v - V_{k,l}) \tag{4.1}$$

where $\mathbf{x} = (x, y)$ and $\mathbf{v} = (u, v)$. So the moments are

$$M_{m,n} = \sum_{k=1}^{2} \sum_{l=1}^{2} w_{k,l} U_k^m V_{k,l}^n = \sum_{k=1}^{2} \rho_k U_k^m \sum_{l=1}^{2} \rho_{k,l}^c V_{k,l}^n = \sum_{k=1}^{2} \rho_k U_k^m \{V_k^n\} \tag{4.2}$$

where $\{V_k^n\}$ is the conditional moments on direction U_k of order n. As a dimensional splitting is used, the two-dimensions scheme is derived for convection in direction x only. The transport equation for moments is then

$$\partial_t M_{m,n} + \partial_x M_{m+1,n} = 0, \quad m, n \geq 0.$$

As it is demonstrated in one-dimension, the main issue for building a kinetic scheme is to define a conservative reconstruction of the moments. So here we detail the two-dimension reconstruction only, the exact definition of the two-dimension kinetic scheme being easily emphasized from theone-dimensional kinetic scheme of section 3. As in one-dimension, it is not sufficient to add the correction proposed in (Bouchut *et al.* 2003). All y quadrature points are coupled, and furthermore their reconstructions are highly sensitive to the reconstruction of x quadrature. To avoid having to solve such a coupled system, we propose reconstructing the x quadrature (ρ_k and U_k) with the algorithm of subsection 3.2, as the convection is dominated by this quadrature. For the y quadrature, it is interesting to note that conditional moments are passive scalar with respect to x convection. So instead of reconstructing the full quadrature, we proposed to reconstruct the conditional moments, by means of the central conditional moments to ensure that

the reconstruction is realizable:

$$v_k^m(x) = \frac{\{V_k^1\}}{\{V_k^0\}} = \bar{v}_k^m + D_{v_k^m}(x - x_i), \tag{4.3}$$

$$e_k(x) = \frac{\{V_k^2\}}{\{V_k^0\}} - \left(\frac{\{V_k^1\}}{\{V_k^0\}}\right)^2 = \bar{e}_k + D_{e_k}(x - x_i), \tag{4.4}$$

$$\begin{aligned} q_k(x) &= \frac{\left(\{V_k^3\}\{V_k^0\}^2 - \{V_k^1\}^3\right) - 3\{V_k^1\}\left(\{V_k^0\}\{V_k^2\} - \{V_k^1\}^2\right)}{\{V_k^0\}^3} \\ &= \bar{q}_k + D_{q_k}(x - x_i), \end{aligned} \tag{4.5}$$

where the slopes are defined using a minmod limiter. The reconstruction of the conditional moments is then

$$\{V_k^0\} = 1 \tag{4.6}$$

$$\{V_k^1\} = \bar{v}_k^m + D_{v_k^m} x \tag{4.7}$$

$$\{V_k^2\} = \bar{e}_k + (\bar{v}_k^m)^2 + (D_{e_k} + 2v_k^m D_{v_k^m})x + D_{v_k^m}^2 x^2 \tag{4.8}$$

$$\{V_k^3\} = \bar{q}_k + 3\bar{v}_k^m \bar{e}_k + (v_k^m)^3 + x\left(D_{q_k} + 3D_{v_m}\bar{e} + 3D_{e_k}\bar{v}_k^m + 3(\bar{v}_k^m)^2 D_{v_k^m}\right) \tag{4.9}$$

$$+x^2\left(3D_{v_k^m}D_{e_k} + 3D_{v_k^m}^2\bar{v}_k^m\right) + x^3 D_{v_k^m}^3 \tag{4.10}$$

Thus the conditional moments are now polynomials functions $\{V_k^n\} = \sum_{p=0}^{n} \alpha_p^{k,n} x^p$. Under the constraints that $M_{0,n}$ and $M_{1,n}$ are conserved, the algorithm gives three 2×2 linear systems to solve for each n:

$$M_{0,n} = \sum_{k=1}^{2}\sum_{p=0}^{n} A_{k,p}\alpha_p^{k,n} \ , \ M_{1,n} = \sum_{k=1}^{2}\sum_{p=0}^{n} B_{k,p}\alpha_p^{k,n}, \tag{4.11}$$

where:

$$A_{k,p} = \frac{\Delta x^p}{2^{p+1}}\left[\bar{\rho}_k \frac{\left(1-(-1)^{p+1}\right)}{(p+1)} + D_{\rho_k}\Delta x \frac{\left(1-(-1)^{p+2}\right)}{2(p+2)}\right] \tag{4.12}$$

$$B_{k,p} = \bar{U}_k A_{k,p} + \frac{\Delta x^p D_{U_k}}{2^{p+1}}\left[\bar{\rho}_k \Delta x \frac{\left(1-(-1)^{p+2}\right)}{2(p+2)} + D_{\rho_k}\Delta x^2 \frac{\left(1-(-1)^{p+3}\right)}{2^2(p+3)}\right]. \tag{4.13}$$

For $n = 1$, a linear system on $\bar{v}_1^m$ and $\bar{v}_2^m$ is obtained. For $n = 2$, the linear system is on $\bar{e}_1$ and $\bar{e}_2$ and depends on $\bar{v}_1^m$ and $\bar{v}_2^m$, which are already found. For $n = 3$, the linear system on $\bar{q}_1$ and $\bar{q}_2$ depends on $\bar{v}_1^m$, $\bar{v}_2^m$, $\bar{e}_1$, and $\bar{e}_2$, which are also already defined by the two previous systems. So the reconstruction is fully defined, and we just have to use the kinetic scheme to evaluate the fluxes.

The proposed reconstruction ensures the realizability of the moments. For the maximum principle, we still have to provide a potential extra limitation in order to ensure the maximum principle in the y direction for the abscissas. Whereas it is shown in the following that the method provides excellent results in the proposed test case, we still have to provide a firm mathematical background as well as further studies in order to deal with such a second-order reconstruction at the frontier of the moment space for both smooth and singular solutions. Indeed it has been shown in Chalons *et al.* (2011*b*)

that the numerical scheme should preserve a cone in the (e, q) phase plane in order to be consistent with the original system of PDEs.

5. Results and discussion

5.1. *Order accuracy study*

The first series of test cases assesses the second-order numerical accuracy in space and time of the scheme presented in section 3.2. This result is based on a simple one-dimensional case for which an analytical solution exists. L_1 errors relative to the analytical solution are calculated for each moments. These errors are computed for three schemes: first and second order, and also the scheme presented in (Vikas *et al.* 2011) which is only partially second order. The initial weight and abscissa fields are given by

$$\begin{cases} \omega_1 = \exp\left(\dfrac{(x-0.5)^2}{\sigma^2}\right), U_1 = 0.5 + 0.5x, \quad \omega_2 = 0, U_2(x) = 0, x < 1, \\ \omega_1 = 0, U_1(x) = 0, \quad \omega_2 = \exp\left(\dfrac{(x-1.5)^2}{\sigma^2}\right), U_2 = -1 + 0.5(x-1), x > 1, \end{cases}$$

where $\sigma = 0.1$. The initial conditions are displayed in Fig. (1)-left. The fact that both fields are not constant enables us to evaluate the reconstruction done by each of the second order schemes. The kinetic solution of this problem is such that the two initiated clouds cross each other so that the dynamics of each cloud is independent from the other. Meanwhile, given the initial velocity profile, they are expanding waves. Indeed their density decreases at a rate proportional to the velocity gradient, see Fig. (1). The final and plotted reconstruction is chosen at time $t = 0.5$.

Numerically, the CFL number is set to 1, and computations are run for $25, 50, 100, 200$ cell grids. An issue already studied in (Chalons *et al.* 2011*b*) has to be tackled in order to reproduce the kinetic solution. Considering velocity gradients inevitably introduces numerical diffusion at points where $|U| < U_{max}$. This means that, if the velocity distribution was mono-modal at these points, one convection step introduces a bi-modal distribution through numerical diffusion. The smaller the gradient is, the closer the abscissas are. In the case studied in (Chalons *et al.* 2011*b*) as well as in this present case, the abscissas difference is negligible, but still exists. This velocity dispersion concerns both clouds of this test case. However the four-moment quadrature can describe only two abscissas at the most. Therefore, when both clouds cross, the four-node resulting distribution is projected on a two-node distribution. This creates singularities, called δ-shocks in the context of kinetic methods, characterized by important density concentration.

To prevent δ-shock from occurring in this case, a criteria is introduced in order to nullify the velocity dispersion (which is accounted for by $M_2 - M_1^2/M_0$) due to numerical diffusion, which is neglibible compared with the dispersion due to the clearly distinct cloud velocity values when clouds cross. Therefore, the small parameter ϵ, introduced in (Chalons *et al.* 2011*b*) in order to discriminate between a one-abscissa and a two-abscissa quadrature, is set as low as possible to fulfill this objective while not impacting the cloud dynamics. An empirical relation that has been proven to work is $\epsilon = \frac{\Delta x^2}{2}$. Nevertheless, being able to a priori set the value of ϵ given the mesh resolution and the velocity gradients is still an area of research. Another potential way to circumvent this issue is to consider a further level of bi-modal quadrature where two Gaussian distributions are reconstructed instead of two Dirac distributions, see (Chalons *et al.* 2011*a*).

Results of the grid convergence study are displayed in Table (1), Fig. (2) and Fig. (3).

Scheme	First order	Second order from (Vikas *et al.* 2011)	Second order
m_0	0.88	1.03	1.52
m_1	0.93	1.09	1.49
m_2	0.89	1.08	1.53
m_3	0.93	1.04	1.5

TABLE 1. L_1 error and numerical order of accuracy of the three tested schemes.

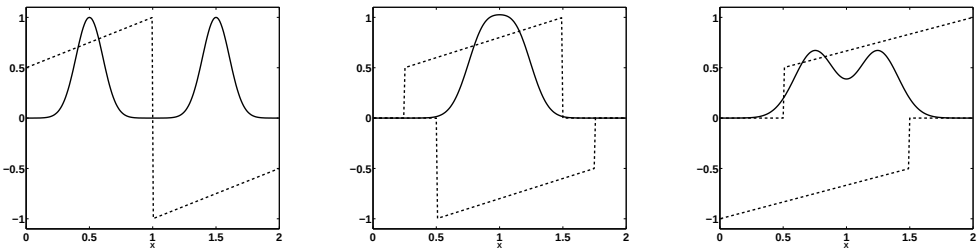

FIGURE 1. Dynamics of two crossing clouds in terms of weights (solid line) and abscissas (dashed line). Left: Initial conditions; Middle: solution at $t = 0.5$; Right: solution at $t = 1$.

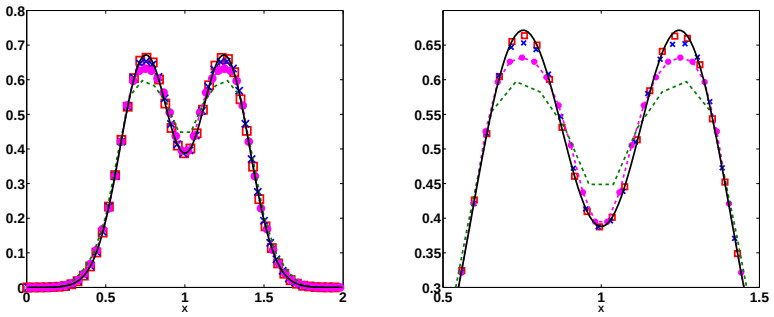

FIGURE 2. Dynamics of two crossing clouds in terms of weights at $t = 1$. Left: Analytical solution (solid line), and numerical solutions for a 200 (squares), 100 (crosses), 50 (circles) and 25 (dashed line) cell grid. Right: Focus on the interest zone

The principal conclusion is that the numerical order of our scheme is close to the theoretical second-order. For example, if we consider the density, the numerical order is 1.52, i.e., 1.73 times the numerical order for the first-order scheme. This study secondly shows that the scheme designed in (Vikas *et al.* 2011) has an accuracy order much closer to one, but involves a simpler algorithm.

5.2. *Dynamics of colliding jets*

This second one-dimensional test case emphasizes the importance of having an accurate transport scheme, in order to stay close to the kinetic solution. Whereas the initial fields

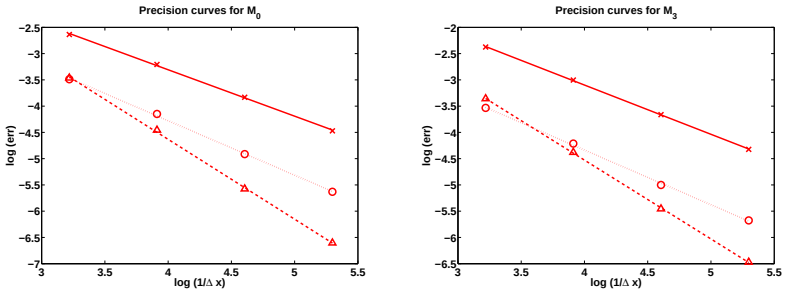

FIGURE 3. Error curves with respect to grid refinement in logarithmic scale: first order scheme (solid line), partially and fully second order scheme (dotted and dashed line). Left: results for M_0; Right: results for M_3.

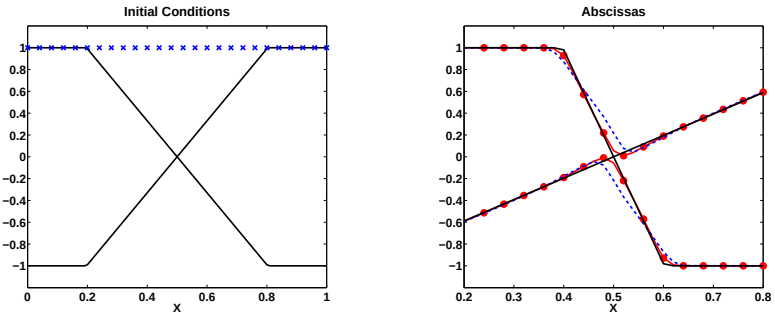

FIGURE 4. Dynamics of colliding jets. Left: Initial conditions for abscissas (solid line) and weights (crosses). Right: Results at $t = 0.2$ for abscissas (right). Analytical solution (solid line), second order solution (crosses), partially second order solution (dashed line).

or weights are $\omega_1 = \omega_2 = 1$, those for the abscissas write

$$\begin{cases} U_1(x) = 1, & U_2(x) = -1, & x < 0.2, \\ U_1(x) = -2/0.6(x - 0.2), & U_2(x) = -1 + 2/0.6(x - 0.2), & 0.2 < x < 0.8, \\ U_1(x) = -1, & U_2(x) = 1, & x > 0.8, \end{cases} \tag{5.1}$$

and are shown in Fig. (4)-left. Given the negative slope of U_1, the first quadrature node is a compaction wave, meaning that ω_1 is increasing in areas of negative gradient of U_1, whereas the second quadrature node is an expansion wave, with ω_2 decreasing in areas of positive gradients of U_2. Fig. (4)-right, (5), and (6) displays the kinetic solution at time $t = 0.2$ (black curve), focusing on the center of the domain, which is the interest zone. Two numerical solutions are displayed, given by the second-order scheme presented here and the partially second-order scheme of (Vikas *et al.* 2011).

Let us remark that this case is symmetrical to the one-dimensional cases studied in (Vikas *et al.* 2011), where the fields of velocity are assumed constant, and the fields of weights are initiated with gradients. The computation is performed with a CFL equal to one, in a 50-cell grid. At the domain center, as in the previous case, numerical diffusion leads to a tri-modal distribution, thus creating a δ-shock. More precisely, two δ-shocks are created, transported with the velocity resulting from the two node quadrature of the initial tri-modal distribution. These singularities correspond to the two pics observed in Fig. (6)-left at the domain center. Because the second-order scheme reduces numerical diffusion, these singularities, although existing, are considerably attenuated.

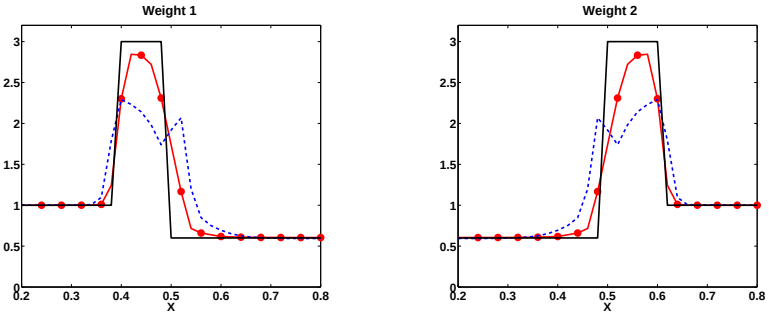

FIGURE 5. Dynamics of colliding jets, at $t = 0.2$ for ω_1 (left) and ω_2 (right). Analytical solution (solid line), second order solution (crosses), partially second order solution (dashed line).

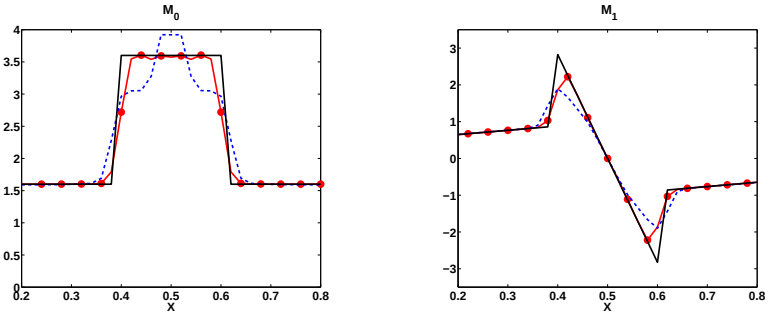

FIGURE 6. Dynamics of colliding jets, at $t = 0.2$ for M_0 (middle) and M_1 (right). Analytical solution (solid line), partially and fully second order solution (crosses and dashed line).

This difference of accuracy is also highlighted in Fig. (5) representing the weights and in Fig. (4)-right representing the abscissas at time $t = 0.2$. This case is complementary to the first case where regular solutions were studied and in this case, the accuracy of the partially second-order scheme is of same order as our second-order scheme for a coarse mesh (≤ 50 cells). When singularities occur, the accuracy enhancement of the second-order scheme is shown to be a real asset and leads to results much closer to the analytical solution than the partially second-order scheme, even for coarse grids.

5.3. *Two-dimensional case*

This two-dimensional case is based on the same x velocity and density profiles for the x quadrature as in subsection 5.2, with $\rho_1 = \rho_2 = 1.0$. For the y quadrature, $\rho_{1,1} = \rho_{2,2} = 0.7$ and $\rho_{1,2} = \rho_{2,1} = 0.3$, and

$$\begin{cases} V_1(x) = 1, & V_2(x) = -1, & x < 0.2, \\ V_1(x) = 1 - 2/0.6(x - 0.2), & V_2(x) = -1 + 2/0.6(x - 0.2), & 0.2 < x < 0.8, \\ V_1(x) = -1, & V_2(x) = 1, & x > 0.8. \end{cases} \tag{5.2}$$

The solution is homogeneous in the y direction, so the transport is solved for x direction only. For the partially second-order scheme, we also use the linear reconstruction of the conditional moments. Results are shown on Fig. 7 for CFL = 1 and with 50 cells. Concerning the x quadrature (M_{00}, M_{10}, and abscissas), previous results are retrieved, as they are independent of the y quadrature which is seen as a passive scalar. For the

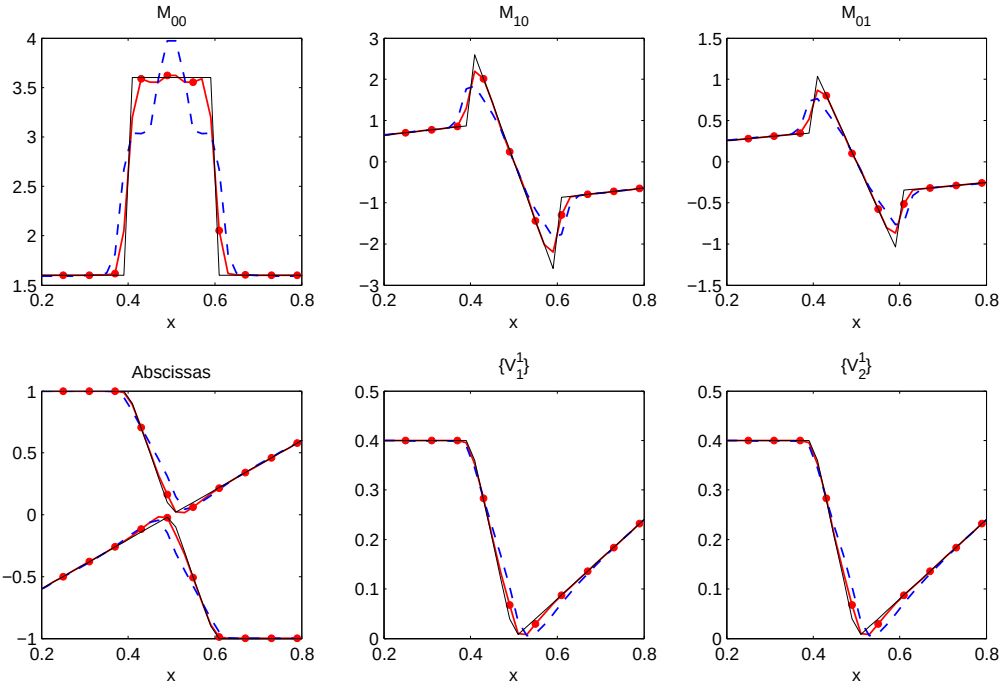

FIGURE 7. Dynamics of colliding jets in two-dimensions, homogeneous in y direction: moments M_{00}, M_{10}, M_{01}, x abscissas, $\{V_1^1\}$, $\{V_2^1\}$ at $t = 0.2$ for the analytical solution (solid line), the partially second order scheme (dashed line), and the fully second order scheme (line with circle).

y quadrature, we can see that moment M_{01} (which depends on the weights of the x quadrature, and the y quadrature) is also sensitive to our reconstruction strategy. The pure V moments are also sensitive to the reconstruction, this sensibility being either due to the convection of those moments as a passive scalar with respect to the x velocity, or the reconstruction of the conditional moments. So we demonstrate that fully reconstructing the quadrature in the convection direction is mandatory and also important if we want to reproduce the moments in other directions, as they are highly coupled to the reconstruction in x direction.

6. Conclusion and perspectives

A fully second-order scheme for a high-order moment method is presented. It relies on the quadrature method explained in (Chalons *et al.* 2011*b*) and (Yuan & Fox 2011). The proposed scheme is designed so that the maximum principle for velocity abscissas and moment conservation is enforced despite the strongly nonlinearity involved. Its second-order numerical accuracy is assessed and proves to be highly beneficial compared to first order or partially second order schemes. In the perspective of extending this scheme to multi-dimensional configurations, the ability of the scheme to capture moment dynamics is proven on a preliminary two-dimensional test case, paving the way for further developments. We still need a detailed study at the boundary of the moment space, especially in the framework of the multi-dimensional quadrature, as well as a further optimization of the proposed algorithms. Moreover, an interesting perspective consists in applying the ideas developed here to multi-Gaussian reconstruction of velocity distributions in-

troduced in Chalons *et al.* (2011*a*). This type of model is more complex but has the advantage of preventing unphysical δ-shock occurrence. It naturally yields a powerful tool for the large eddy simulation of particle flows by accounting for a subgrid velocity dispersion in addition to the ability of allowing the particle trajectory crossing.

Acknowledgments

Support from CTR and from RTRA DIGITEO (Project MUSE, PI M. Massot) and Ecole Centrale Paris for A. Vié's Post-doctoral fellowship are gratefully acknowledged.

REFERENCES

Bouchut, F., Jin, S. & Li, X. 2003 Numerical approximations of pressureless and isothermal gas dynamics. *SIAM J. Numer. Anal.* **41** (1), 135–158.

Brenier, Y. & Grenier, E. 1998 Sticky particles and scalar conservation laws. *SIAM Journal of Numerical Analysis* **35**, 2317–2328.

Chalons, C., Fox, R. O. & Massot, M. 2011*a* A multi-Gaussian quadrature method of moments for gas-particle flows in a LES framework. In *Proc. of the 2010 Summer Program, Center for Turbulence Research, Stanford University*, pp. 347–358.

Chalons, C., Kah, D. & Massot, M. 2011*b* Beyond pressureless gas dynamics: quadrature-based velocity moment models. *Communication in Mathematical Sciences (accepted for publication, in revision)* pp. 1–21, available online at http://hal.archives-ouvertes.fr/hal-00535782/en/.

Desjardin, O., Fox, R. & Villedieu, P. 2008 A quadrature-based moment method for dilute fluid-particle flows. *J. Comput. Phys.* **227**, 2514–2539.

Gosse, L., Jin, S. & Li, X. 2003 On two moment systems for computing multiphase semiclassical limits of the Schrödinger equation. *Math. Model Methods Appl. Sci* **13**, 1689–1723.

Jin, S. & Li, X. 2003 Multi-phase computations of the semiclassical limit of the Schrödinger equation and related problems: Whitham vs Wigner. *Physica D: Nonlinear Phenomena* **182** (1-2), 46 – 85.

Kah, D. 2010 Taking into account polydispersity for the modeling of liquid fuel injection in internal combustion engines. PhD thesis, Ecole Centrale Paris.

Kah, D., Laurent, F., Fréret, L., de Chaisemartin, S., Fox, R., Reveillon, J. & Massot, M. 2010 Eulerian quadrature-based moment models for polydisperse evaporating sprays. *Flow, Turbulence and Combustion* **85** (3-4), 649–676.

Massot, M., Laurent, F., de Chaisemartin, S., Fréret, L. & Kah, D. 2009 Eulerian multi-fluid models: modeling and numerical methods. In *Modelling and Computation of Nanoparticles in Fluid Flows*, pp. 1–86. NATO RTO-EN-AVT-169, available at http://www.rta.nato.int/Pubs/RDP.asp?RDP=RTO-EN-AVT-169.

Runborg, O. 2000 Some new results in multiphase geometrical optics. *M2AN. Mathematical Modelling and Numerical Analysis* **34**, 1203–1231.

Vikas, V., Wang, Z., Passalacqua, A. & Fox, R. O. 2011 Realizable high-order finite-volume schemes for quadrature-based moment methods. *Journal of Computational Physics* **230** (13), 5328 – 5352.

Williams, F. A. 1958 Spray combustion and atomization. *Phys. Fluids* **1**, 541–545.

Yuan, C. & Fox, R. 2011 Conditional quadrature method of moments for kinetic equations. *Journal of Computational Physics* pp. 8216–8246, to appear.